Yoshida, H., et al., "Heat Transfer Between a Wall Surface and a Fluidized Bed," *Intern. J. Heat Mass Transfer*, 12, 529-526 (1969).
Zamir, M., and A. D. Young, "Experimental Investigation of the Boundary Layer in a Streamwise Corner," *Aero. Quart. J.*, 313-339 (1970).
Ziegler, E. N., et al., "Effects of Solid Thermal Properties on Heat Transfer to Gas Fluidized Beds," *Ind. Eng. Chem. Fundamentals*, 3, 324-328 (1964).

Manuscript received July 5, 1978; revision received October 13, and accepted November 13, 1978.

Turbulence Characteristics and Mass Transfer at Air-Water Surfaces

JOHN T. DAVIES
and
FRANCISCO J. LOZANO
Department of Chemical Engineering
University of Birmingham
Birmingham B15 2TT
England

The turbulence intensities and spectra in water very close to an air interface have been measured with a hot wire anemometer. The turbulence in the water has been induced in three ways: with a stirrer, by a submerged jet, and by flow of a thin film of water over inclined plates, both rough and smooth.

We find that the root-mean-square fluctuation velocity $\tilde{v_x}'$ shows for the first system no regular trend with the distance y below the surface, while for the second system $\tilde{v_x}'$ increases markedly as the surface is approached. In water films over the rough plates, $\tilde{v_x}'$ can be as high as four times the shear stress velocity.

The turbulence energy spectra close to the surfaces in the first and second systems show (Figure 6) no extended region of slope $-5/3$, whereas for flow over the plates, there is an appreciable subrange of this slope (Figures 8 and 9).

Intensities of turbulence in the surface region are as high as 30 to 50% in the first system, up to 100% in the second system, and 17% over smooth plates and up to 60% over rough plates.

These turbulence characteristics can be related to the rates of mass transfer for oxygen absorbing into water by comparing plots of $k/D^{1/2}$ with the square roots of the different eddy frequencies. The Levich treatment [interpreted by Equation (15)] gives good agreement with the stirred cell and jet results. For the smooth and rough plates, mass transfer depends on eddies intermediate in size between the x directional and the y directional large eddies. In all cases, the Kolmogoroff eddy frequencies are much too high to correlate with mass transfer rates.

Further, the energy spectra show that 60 to 80% of the total eddy energy lies in the larger eddies, with only 1% (or less) in the Kolmogoroff range.

We conclude that the Prandtl sized eddies, and even larger eddies, determine mass transfer rates at a free surface.

Direct measurement of concentration fluctuation frequencies, using platinum microelectrodes, was found to be unsatisfactory because of the poor frequency response of the amplified signals.

SCOPE

The distribution of the sizes and energies of eddies very close to an air-water surface are measured in different turbulent systems: stirred cells, water jets impinging from below on to a free surface, and thin films of water flowing over smooth and rough plates. The fluctuation velocities, important in mass transfer at free surfaces, were also measured.

The experimental method is to position a hot wire anemometer closely below the free surface. The results were analysed using a Hewlett-Packard correlator.

To determine what sized eddies at a free liquid surface are primarily responsible for mass transfer, the turbulence characteristics are compared with mass transfer coefficients measured for the absorption of oxygen into water.

Previously published theoretical treatments have assumed that either the very large or the very small eddies are dominant in mass transfer at free surfaces. The present work decides this question experimentally.

Correspondence concerning this paper should be sent to John T. Davies. Francisco J. Lozano is with Facultad de Quimica, Universidad Nacional Autonoma de Mexico, Mexico D.F.

0001-1541-79-2309-0405-$01.25.

CONCLUSIONS AND SIGNIFICANCE

For a stirred cell, the root mean square fluctuation velocity in the plane of the surface $\tilde{v}_x'$ is independent of Re at low stirring speeds, as assumed by Levich. At higher Re values, however, swirl effects cause positive and negative deviations. For the impinging submerged jets, both $\tilde{v}_x'$ and the mean velocity $\bar{v}_x$ increase markedly as the interface is approached. In both systems, the intensity of turbulence near the surface was surprisingly great (~50%).

Within thin films of water flowing over an inclined smooth plate, the intensity of turbulence was lower (~17%); with a base plate with large scale roughness elements to cause wake interference flow, the intensity reached 60% in certain positions. If the shear stress velocity is v_o, the data give $\tilde{v}_x'/v_o = 1.17$ for the smooth plate, though $\tilde{v}_x'/v_o$ can be as high as 4.1 for flow over the rough plate. The latter figure confirms calculations based on the previously published high rates of gas absorption when there is wake interference flow.

The x directional energy spectra show that, even close to the surface, large eddies contain most of the turbulence energy. For flow over the plates, there is an extended region of slope −5/3 (Figures 8 and 9), indicating an inertial subrange of decaying eddies.

Comparisons of $k/D^{1/2}$ with the square roots of the various eddy frequencies show that the Levich treatment based on Prandtl sized eddies [Equation (15)] gives good agreement with experiment for stirred cells and impinging submerged jets.

For thin films of water flowing over rough and smooth plates, the eddies responsible for mass transfer are intermediate in size between the x directional and the y directional large eddies.

In all cases, the very small (Kolmogoroff) eddies are unimportant, as is shown both by their very high frequencies and also by our finding that only 1% or less of the total eddy energy lies in the Kolmogoroff range.

Prandtl sized eddies, and even larger eddies, are thus responsible for mass transfer at a free surface.

Direct measurement of concentration fluctuation frequencies is shown to be unsatisfactory because of the poor frequency response of the amplified signals.

The investigation was designed to answer experimentally three questions:

1. How do the velocity fluctuations in the x direction (in the plane of the surface) change as the surface of a liquid is approached?
2. How do the velocity fluctuations relate to the shear stress velocity v_o for liquid films flowing over plates?
3. Which sized eddies are most important in mass transfer at free liquid surfaces?

The answer to the first question is important in theories of mass transfer at free surfaces. It is widely accepted that some tangential turbulent fluctuations v_x' persist right into the plane of a clean gas-liquid surface when the liquid is turbulent, but the further assumption that v_x' remains constant as the interface is approached (that is, as $y \to 0$) is basic to some recent work (Levich, 1962; Davies, 1972) on mass transfer. The condition that v_x' is independent of y as $y \to 0$ gives, in conjunction with the continuity equation, the relations

$$\tilde{v}_y' \propto y \tag{1}$$

and hence

$$D_E \propto y^2 \tag{2}$$

Previous work on restrained turbulent jets of liquids in air (Davies, 1972) shows that the collisions of the liquid eddies with the surface are largely (~94%) elastic; that is, most of the eddies are bounced back into the bulk by surface tension. That only about 6% of the eddy collisions with the surface are inelastic (leading to surface renewal by lateral spreading in the plane of the surface) suggests that $\tilde{v}_x'$ close to the surface will be only slightly augmented.

In the present work, we study how $\tilde{v}_x'$ varies with y close to the free surface for both stirred cells and for impinging submerged jets.

The second question is answered, for water films flowing over smooth and rough plates, by direct measurements of $(\tilde{v}_x'/v_o)$ as close as possible to the free surface. Earlier work (Davies, 1972) had suggested indirectly (from mass transfer rates) that this velocity ratio was somewhat greater than unity for the smooth plate and considerably greater (about 4) for the rough plates. A more direct confirmation of this is therefore desirable.

The third question can be answered only by knowing the distribution of energies in the different eddy size ranges, very close to the free surface. Many purely theoretical treatments of mass transfer at gas-liquid surfaces have appeared in recent years, based on various assumptions about which eddies are mainly responsible for promoting mass transfer in the surface region of the turbulent liquid. However, with some additional assumptions and a few arbitrary constants, all the mass transfer theories can give reasonable agreement with experimental data.

SMALL EDDY MODELS

Small eddies, in the Kolmogoroff range (tens of micrometers), are the basis of the theories of mass transfer of Ruckenstein (1967), Banerjee, Scott, and Rhodes (1968), Miyauchi and Kataoka (1970), Lamont and Scott (1970), Kataoka and Miyauchi (1972), Prasher (1973), and Prasher and Wills (1973).

These Kolmogoroff eddies are related to the kinematic viscosity ν of the liquid, and the small eddy models predict that the mass transfer coefficient varies as $k \propto \nu^{-1/4}$.

LARGE EDDY MODELS

Larger eddies, in the Prandtl size range, were assumed by Levich (1962) and by Davies (1972) to be dominant in controlling mass transfer rates at liquid surfaces. This was supported by the work of Kataoka and Miyauchi (1972). For liquid-liquid interfaces, in vessels stirred by a blade of length L, an eddy size of 0.3 L gives good agreement with experiment (McManamey et al., 1973; McManamey et al., 1975).

For thin films of water flowing over rough plates, Brumfield, Houze, and Theofanous (1975) used the macroscale eddy length l_L in the interpretation of the mass transfer results, defining this eddy length in such a manner that it decreased as Re increased.

For gas absorption into turbulent liquid downstream of a grid, Fortescue and Pearson (1967) used a large eddy model, visualizing the eddies as roll cells sweeping fresh liquid to and along the surface, thus renewing it. They used a value of l_L of 5 mm, independent of the velocity of the stream of water, and depending only on the geometric parameters. This leads to a dependence of k (the mass transfer coefficient on the liquid side) on $Re^{0.5}$, though this low power dependence has been ascribed (Davies, 1972) to a low grid Reynolds number in these experiments, resulting in essentially a collection of separate laminar circulation cells rather than true (that is, chaotic) turbulent motion.

Large eddy models predict that k is independent of ν.

EXPERIMENTAL STUDIES ON EDDIES NEAR FREE SURFACES

Jeffries, Scott, and Rhodes (1969) used hot film probes to study eddy viscosities near the surface in relation to wind generated waves on a water surface. Kataoka and Miyauchi (1972) used a hot wire probe to study turbulence at free surfaces but could not measure frequencies greater than 50 Hz. They were not able to decide whether the large or small eddies were dominant in mass transfer.

Bungay, Huang, and Sanders (1973) measured concentration fluctuation frequencies close to the surface of a stirred vessel using a small, oxygen sensitive electrode, but their equipment measured only those eddy frequencies lower than 15 Hz. Moreover, for their stirred cell system, with oxygen absorbing into water, their experimental figures lead to anomalously low diffusivities D (between 2 and 20% of those generally accepted). Tsao and Lee (1975) used a similar technique, finding D apparently less than 20% of the accepted value. Clearly, such measurements are suspect.

The object of the present work is to compare eddy frequencies with the experimental mass transfer coefficients and thus to decide directly which eddy sizes are responsible for most of the mass transfer.

THEORETICAL

To derive the eddy length scales from the measured time scales, Taylor's hypothesis (1938) is used. He assumed that at a fixed point the sequence of time delays t (due to the fluctuating eddy velocities) is equivalent to eddy separation distances of $\bar{v}_x t$. In practice, Taylor's hypothesis requires a slight correction, (Lumley, 1965) for the intensity of turbulence, and the measured values of $(\widetilde{\partial v_x'/\partial t})$ are accordingly connected to $(\widetilde{\partial v_x'/\partial x})$ by division by $\bar{v}_x$ and then corrected by Lumley's factor.

The Eddy Microscale l_m (Taylor Microscale)

The length l_m of small eddies (at the upper end of the energy dissipating eddy scale) is defined by

$$l_m = 2^{1/2} [\widetilde{v_x'}/(\widetilde{\partial v_x'/\partial x})] \tag{3}$$

The Eddy Macroscale l_L (Integral Length)

This scale is derived from the velocity fluctuation autocorrelation coefficient $Q(t)$, which for convenience is normalized with respect to $(\widetilde{v_x'})^2$ to give a function designated $Q^*(t)$. The integral of this gives a macro-time scale t_L for the eddies

$$t_L = \int_0^\infty Q^*(t)\,dt \tag{4}$$

Thus, t_L is the time over which an observed fluctuation v_x' is correlated with itself; that is, it is the lifetime of the larger (energy containing) eddies.

Numerical integration of Equation (4) gives t_L, and hence the integral eddy length scale l_L is obtained using Taylor's hypothesis:

$$l_L = \bar{v}_x t_L \tag{5}$$

Energy Spectra

To obtain the distribution of energy in the variously sized eddies, one uses the autocorrelation $Q^*(t)$, which has its Fourier transform in the spectrum of frequencies f. The Fourier transform of $Q^*(t)$ was obtained numerically, full details being available (Lozano, 1976). This procedure gives the normalized one-dimensional frequency energy function $\phi^*(f)$, in units of seconds. From this, by application of Taylor's hypothesis, one obtains ψ^*, the normalized energy function:

$$\psi^* = \bar{v}_x \phi^* \tag{6}$$

The unnormalized energy function ψ is related to the normalized function by

$$\psi^* = \frac{\psi}{(\widetilde{v_x'})^2}$$

and the units of ψ are $m^3 \cdot s^{-2}$. Both ψ and ψ^* are functions of the eddy size l but are more conveniently plotted against κ, the eddy wave number, where κ is defined as $2\pi/l$. Further, the integral of ψ with respect to κ is the kinetic energy per unit mass; that is, the energy in the band of eddy wave numbers around κ is ψ times the width of the chosen band.

It is known (for example, Tennekes and Lumley, 1972) that if there is an inertial subrange of eddies

$$\psi = 1.5\, P_M^{2/3}\, \kappa^{-5/3} \tag{7}$$

To obtain P_M in the surface region, there are two possible expressions:

$$P_M = 15\nu\, (\widetilde{v_x'})^2 l_m^2 \tag{8}$$

and

$$P_M = (\widetilde{v_x'})^3/l_L \tag{9}$$

These do not give the same result in many of our systems, presumably because Equation (8) refers to isotropic conditions which do not occur in the region of an interface. We therefore use the more general Equation (9) (see Tennekes and Lumley, 1972) to obtain P_M, making a correction (Lumley, 1965) for the intensity of turbulence by dividing the P_M values from Equation (9) by $[1 + 5(\widetilde{v_x'}/\bar{v}_x)^2]$.

Kolmogoroff Eddies

These characteristic eddy lengths and velocities can be obtained directly from the local P_M values by the usual expressions (see, for example, Davies, 1972).

Mass Transfer

From the observed rates of oxygen absorption, we calculate frequencies by applying the Danckwerts (1951) equation

$$k = D^{1/2} s^{1/2} \tag{10}$$

The frequencies from Equation (10) can then be compared with the eddy frequencies f from the turbulence studies.

The first method of obtaining f is from the experimental values $\tilde{v}_x'$ and l_L:

$$f_L = (\tilde{v}_x'/l_L)_{y\to 0} \tag{11}$$

This assumes that the x directional macroscale eddies of size l_L are responsible for mass transfer.

The second method utilizes the Prandtl frequencies, which for a stirred cell are reported (McManamey et al., 1973) to be given by

$$f_P = v'/l_P = 0.22\,NL/0.3L = 0.73N \tag{12}$$

where the 0.22 factor is a mean.

For a submerged jet, the Prandtl length is given (Davies, 1972) by

$$l_P = 0.017 \times (\text{distance from nozzle}) \tag{13}$$

and, in the present work, the total distance from the nozzle is (60 + 20) mm at the point of measurement. For the thin films (thickness B_f) of water flowing over the plates, l_P is variously assumed to be B_f, $0.1B_f$, or 0.1 × (roughness height).

The third method is based directly on the Levich treatment and assumes that v_y' in the vicinity of the surface is the velocity actually responsible for mass transfer to the surface. This velocity can be obtained from

$$\tilde{v}_y' = y\left(\frac{\widetilde{\partial v_x'}}{\partial x}\right)_{y\to 0} \tag{14}$$

The measured values of $(\widetilde{\partial v_x'/\partial x})$ are extrapolated to zero y. From $\tilde{v}_y'$, one then obtains the corresponding eddy diffusivity D_E by writing $D_E = \tilde{v}_y' l$. Assuming that the Prandtl sized y directional eddies control mass transfer, one then equates the eddy length l to $0.4y$. Then, putting $y = \delta_2$ for the region very close to the surface within which $D_E \leq D$, one obtains

$$\delta_2 = 1.58D^{1/2}\,[(\widetilde{\partial v_x'/\partial x})_{y\to 0}]^{-1/2}$$

and hence

$$k = \frac{D}{2\delta_2} = 0.32D^{1/2}\left[\left(\frac{\widetilde{\partial v_x'}}{\partial x}\right)_{y\to 0}\right]^{1/2}$$

or

$$f_y = 0.10\left(\frac{\widetilde{\partial v_x'}}{\partial x}\right)_{y\to 0} \tag{15}$$

where subscript y denotes that the frequency derives from $\tilde{v}_y'$.

The fourth method is also based on the Levich treatment (Davies, 1972)

$$k/D^{1/2} = 0.32\rho^{1/2}\sigma_{\text{equiv}}^{-1/2}\,(v')^{3/2} \tag{16}$$

where σ_{equiv} is taken as 72×10^{-3} Nm^{-1}. A larger value of σ (including a term for the gravitational damping of the large eddies at the surface) would reduce the values reported below of $k/D^{1/2}$ from Equation (16).

The velocity v' in Equation (16) is strictly the fluctuation velocity in the y direction, in the vicinity of the surface but not so close that the eddies are damped by the presence of the surface. For the stirred cell, v' can be substituted by various other velocities, that is, by the mean $\tilde{v}_x'$ as measured close to the surface, or by a velocity proportional to NL (that is, to the peripheral velocity of the stirrer blades).

For the turbulent submerged jets, v' in Equation (16) has been replaced by $\tilde{v}_x'$ extrapolated to zero y.

For the water films over the plates, v' is replaced either by the measured $\tilde{v}_x'$ or alternatively, by v_o (the shear stress velocity) given by

$$v_o = (B_f\, g\, \sin\theta)^{1/2} \tag{17}$$

The fifth calculation involves the Kolmogoroff eddies, the frequencies f_K of these being obtained from the standard relation

$$f_K = \tilde{v}_K'/l_K = (P_M/\nu)^{1/2} \tag{18}$$

EXPERIMENTAL

Mean velocities $\bar{v}_x$ and fluctuation velocities v_x' parallel to the free surface were measured with a hot wire anemometer. The wire, supplied by DISA, was platinum plated tungsten 5 μm diameter and 1.0 to 1.5 mm in length. The wire was soldered across the ends of two fine sewing needles of shaft diameter 0.2 mm, tapering over a length of 2 mm to a tip of 0.04 mm diameter. The resistances of the wires when cold were in the range 1.5 to 8 ohms. The thermal time lag of the hot wires immersed in quiescent distilled water was determined by calibration with a 200 Hz square wave, to be about 0.05 ms when the current was 220 mA. In quiescent air it was about 1.5 ms at 80 mA. Full details of the soldering, calibration, and characteristics of the wire are available (Lozano, 1976). With the stirred cell and jet experiments there was no appreciable drift in the electrical properties of the hot wires.

The function relating velocity fluctuation to resistance fluctuation R' is

$$v_x' = \left(\frac{\partial \bar{v}_x}{\partial R}\right) R'$$

Any errors arising from deviations from this simple linear relation are unimportant for the conclusions reached.

The hot wire probes were operated at constant current with a symmetrical bridge and specially constructed amplifier. The velocity fluctuation signals were recorded on a T3000 Racal-

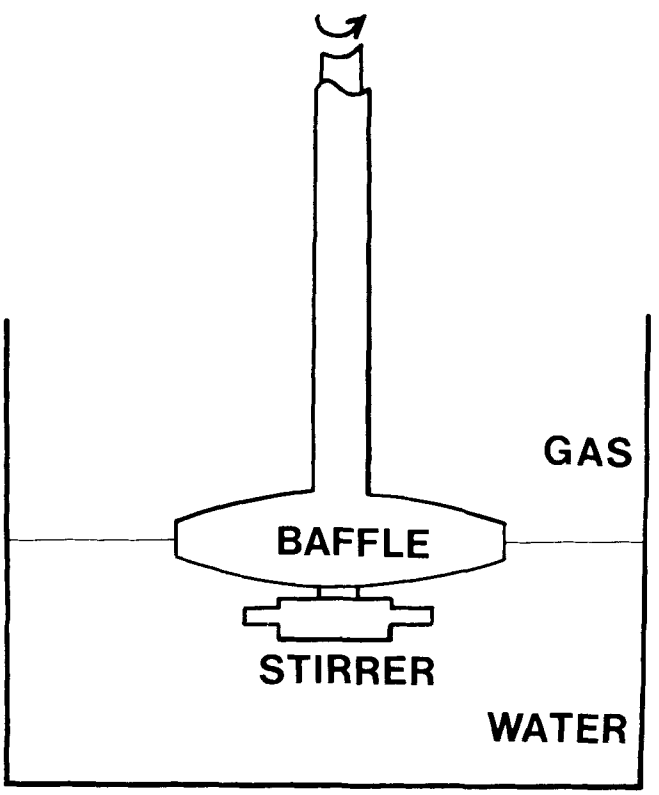

Fig. 1. Stirred cell assembly. Internal diameter of glass cell is 102 mm. Baffle diameter is 45.6 mm. Tip-to-tip length of stirrer is 31.9 mm.

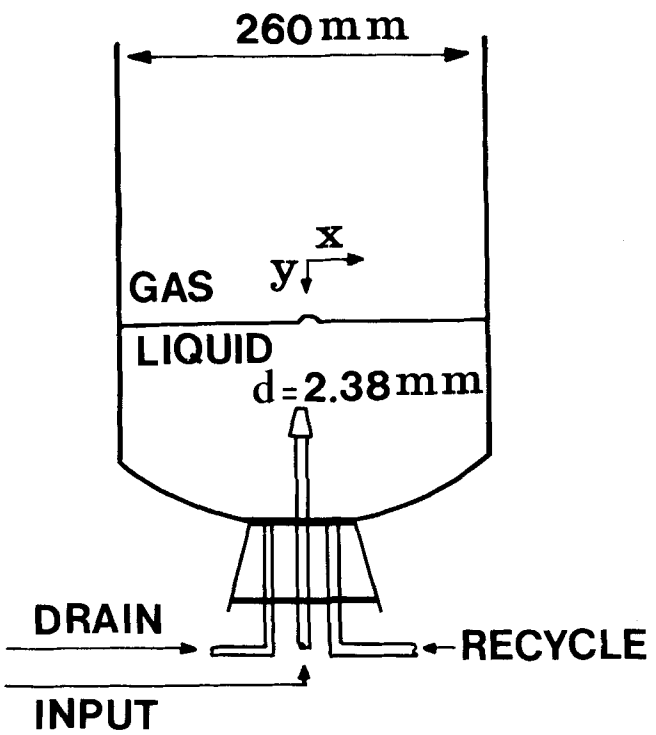

Fig. 2. Submerged jet experiment.

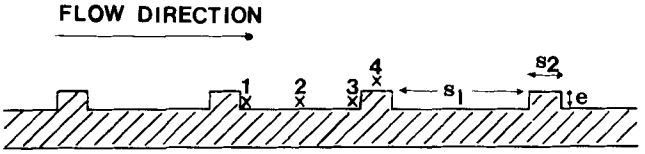

Fig. 3. Part of aluminum plate with large scale roughness elements. Here $s_1 = 12.7$ mm, $s_2 = 3.18$ mm, and $e = 1.91$ mm. Crosses show positions where the turbulence was studied.

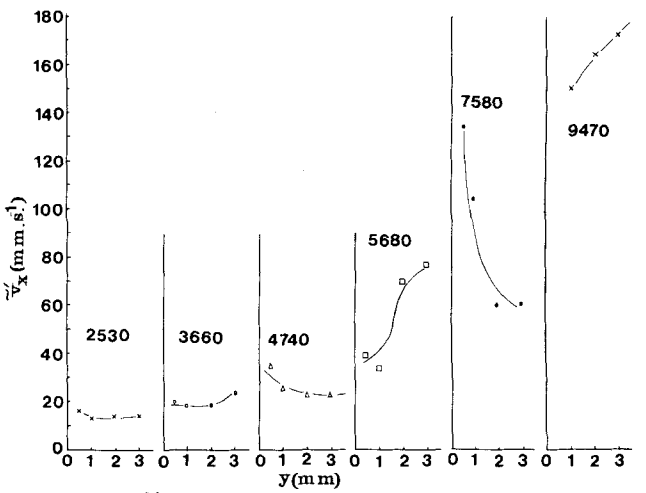

Fig. 4. Plots of $\tilde{v}_x'$ vs. y for the stirred cell at the Reynolds numbers indicated.

Thermionic recorder and processed using a Hewlett-Packard correlator (model 3721) in conjunction with an X-Y recorder.

The hot wires were always set up perpendicular to the flow direction x and parallel with the free surface. Under these conditions, it is known (for example, Hinze, 1975) that it is the x directional fluctuations that are measured.

Freshly distilled water at 25°C was used in all runs with the stirred cell and with the submerged jet. This greatly reduced probe contamination and electrochemical corrosion. But, because of the quantities of water required in the inclined plate experiments, we used tap water passed through a deionizer column and then filtered through a grade A Balston microfiber filter to remove particles above 0.3 μm. In this water, the hot wire anemometer showed a drift in electrical properties, due to corrosion. This drift could be minimized by using lower currents through the bridge (but at the expense of sensitivity), by coating the prongs with polyurethane resin, and by grounding one end of the hot wire to the aluminum of the plate. The drift remaining after these precautions had been taken was linear with time, so that the characteristics of the wire during a run could be easily interpolated.

Stirred Cell

The stirrer assembly and cell are shown in Figure 1. The glass vessel was of 102 mm ID and surrounded by a water jacket to maintain constant temperature. The single, flat bladed stirrer of length 31.9 mm imparted a slow rotation at the interface, enabling the hot wire anemometer to be used to obtain mean velocities in this region. The hot wire probe was inserted through a plastic lid fitted over the cell and was always positioned halfway across the annular space between the central stationary baffle and the wall, with its axis in the radial direction (that is, the rotational liquid flow was across the wire).

Distances of the probe below the surface were 0.5, 1, 2, and 3 mm, these being measured by a cathetometer focusing on a scale on the hot wire support. The zero position was established before the stirrer was turned on and with the wire just touching the water surface. The stirrer and baffle design were such that the surface remained smooth except for slight rippling at the highest stirring rates.

Prior to a run, the cell, the stainless steel stirrer, and baffle were cleaned in chromic acid and rinsed thoroughly. After the cell was filled to the level of the baffle, the free surface was cleaned by sprinkling ignited talc on to the surface and then removing it by suction through a capillary tube.

Impinging Submerged Jet

The apparatus is shown in Figure 2. The water entered the tank through a nozzle of 2.38 mm diameter, situated 60 mm vertically below the surface in the center of the glass cylindrical tank. Distances x in this system were measured radially from the center of the vessel. The bulge on the surface due to jet impingement was less than 10 mm in radius. The hot wire was set with its axis across the direction of flow.

Water Film Over Smooth Inclined Plate

Because of the drift in the hot wire calibration, the electrical current could not be increased to improve the sensitivity. Consequently, turbulence could be detected only at the higher Reynolds numbers.

The aluminum plate, of length 81 cm and width 15 cm, was fixed at 24.3 deg to the horizontal, and the measurements were made halfway along the plate with the wire placed across the direction of flow. The thickness of the water film was about 1 mm, but because of the waves on the surface, the probe position was fixed at 0.5 mm from the plate. The water, purified as above, was fed in over a weir.

Water Film Over Rough Inclined Plate

The roughness elements on the plate (of the same dimensions as the smooth plate) were rectangular projections running across the plate (Figure 3), with geometrical parameters chosen to cause wake interference flow (Davies, 1972) in the water film. The roughness elements were of height $e = 1.91$ mm above the base plate, with $s_1 = 12.7$ mm and $s_2 = 3.18$ mm, these being defined as in Figure 3. The angle of inclination was fixed at 24.3 deg to the horizontal.

The hot wire probe was always fixed at 0.3 mm from the solid surface, this distance being the maximum that allowed operation without intermittent exposures of the hot wire to the air during the turbulent flow across the wire. Turbulence was studied with the probe at positions 1, 2, 3, or 4 (Figure 3).

Mass Transfer Rates

To determine k values, pure oxygen gas was contacted with the turbulent water, and the mean oxygen concentrations in the water at various times were measured with a Beckman 7015A platinum electrode. The plastic end cap of this electrode was replaced by one of stainless steel so that it could be cleaned in chromic acid before each experiment. The electrode required 15 s for 90% response.

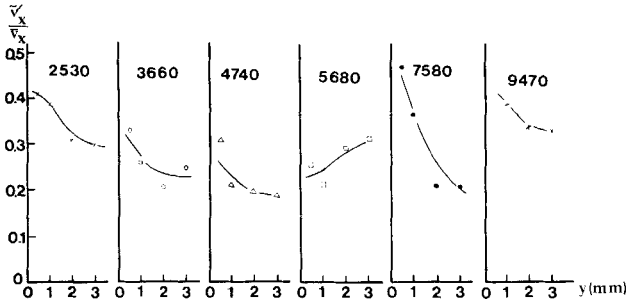

Fig. 5. Plot of $(\tilde{v}_x'/\bar{v}_x)$ vs. y for the stirred cell, at the Reynolds numbers indicated.

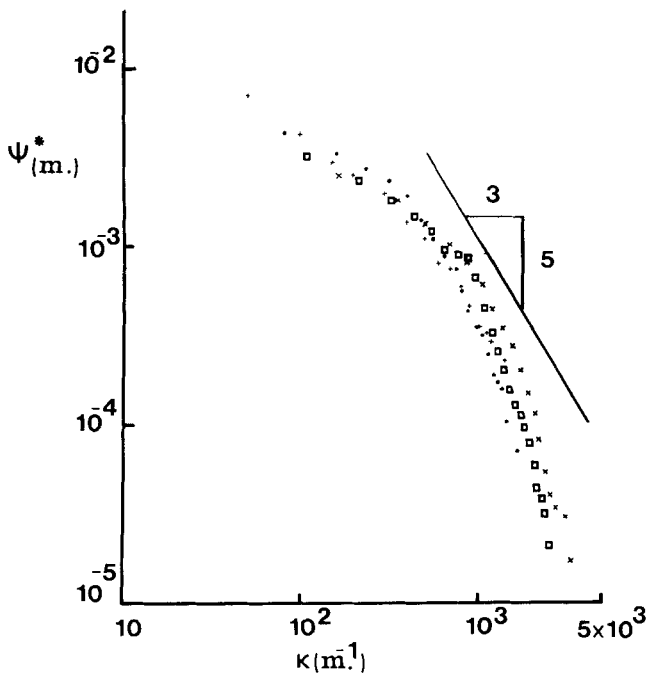

Fig. 6. Normalized wave number spectra of eddies near surface of stirred cell. Here ψ^* is plotted against κ on a log-log scale. Points are as follows: × Re = 2530 with y = 0.5 mm, □ Re = 4 740 with y = 0.5 mm, ● Re = 9 470 and y = 1.0 mm, + Re = 9 470 and y = 3.0 mm. The energy dissipating eddies are those for which $\kappa > 2 \times 10^3$.

Fluctuation concentrations of oxygen were measured with platinum microelectrodes (Transidyne General Corporation), with a special amplifier supplied by the same company. The electrodes had 2 μm tips with 10 μm of exposed platinum. The time for 90% response of the microelectrode signal as amplified was 400 ms, and this could not be reduced because of the very high input impedance required when such a small area of platinum is exposed. We modified the Transidyne amplifier by disconnecting two capacitors which formed a low pass filter at 10 Hz, but frequencies higher than a few Hz were still attenuated, even though some (necessarily inaccurate) frequency components up to 30 Hz could be recorded (Lozano, 1976). With two specially designed amplifiers built in the department, we could not get better results.

RESULTS

Eddies in Stirred Cell

Figure 4 shows that at low Re $(= NL^2/\nu)$, $\tilde{v}_x'$ is virtually independent of Re. At the higher Reynolds numbers, swirls become more pronounced in the flow in the cell, and the Levich assumption that $\tilde{v}_x'$ is independent of y is then not correct everywhere on the surface. Nevertheless, the swirls have both positive and negative effects on $\tilde{v}_x'$ (Figure 4), and there is no general trend as for the submerged jets.

The ratio $\tilde{v}_x'/NL$ is 0.20 ± 0.01 at the four lower Reynolds numbers but rises to 0.47 and 0.56 at the two higher Re values.

The mean local velocity $\bar{v}_x$ decreased slightly towards the interface, while the turbulence intensity $(\tilde{v}_x'/\bar{v}_x)$ increased somewhat (Figure 5), being between 30 and 50% near the surface.

The length of scale l_L (at 0.5 mm below the surface) was in the range 5 to 9 mm, increasing with Re. The length scale l_m was 3 to 5 mm. P_M [defined by Equation

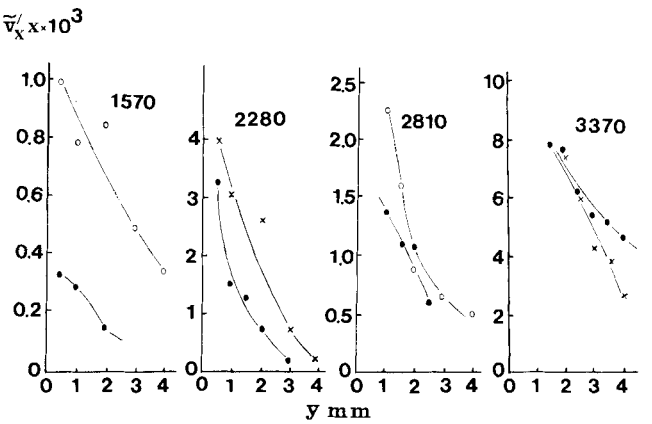

Fig. 7. Plot of $\tilde{v}_x'$ (in m² s⁻¹ × 10³) vs. y for the submerged jet impinging on to a free water surface from inside the water phase at the Reynolds numbers indicated. Points are as follows: ○ x = 10 mm, × x = 15 mm, ● x = 20 mm.

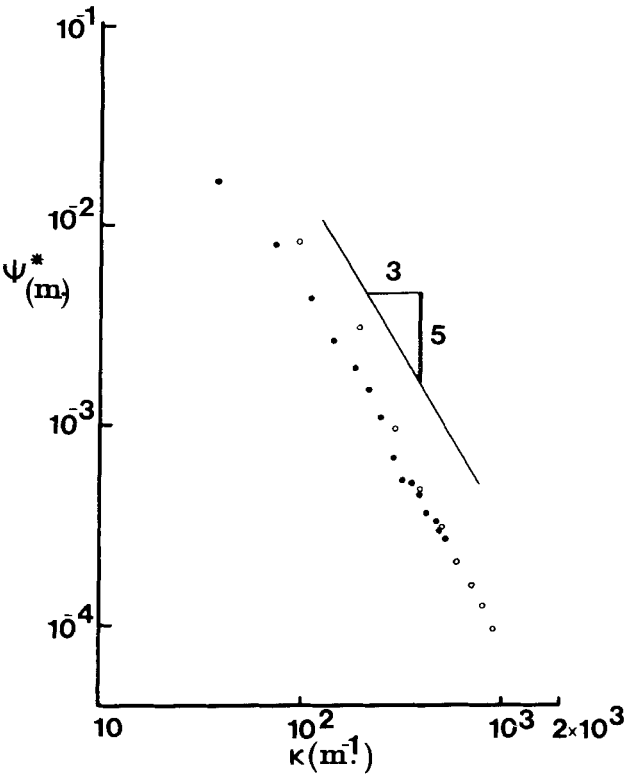

Fig. 8. Normalized wave number spectra of eddies in water films flowing over inclined smooth plate. Here ψ^* is plotted against κ on a log-log scale. Closed circles refer to Re = 1 000, open circles to Re = 1 300. The energy dissipating eddies are those for which $\kappa >$ 10^3.

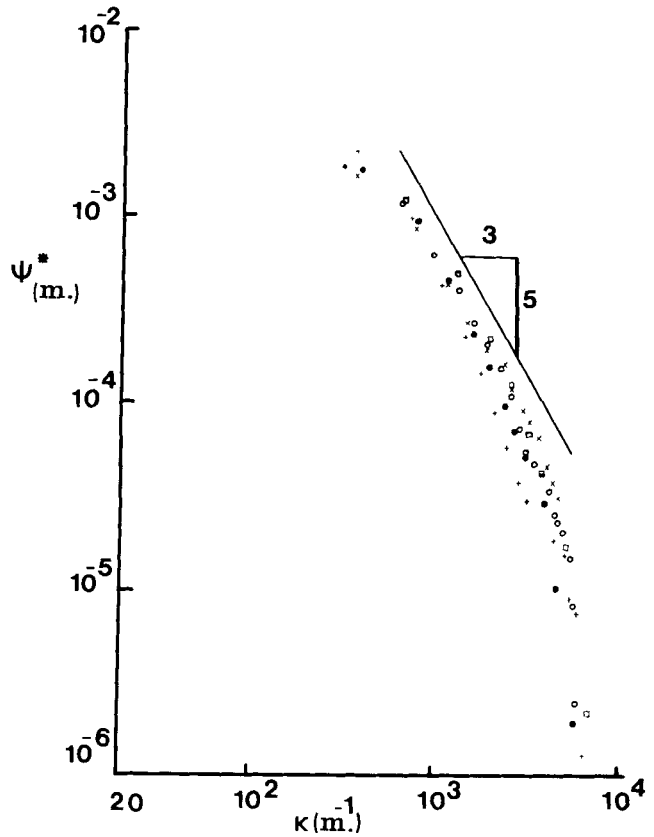

Fig. 9. Normalized wave number spectra for water films flowing over inclined rough plate, plotted as in Fig. 8. The spectra are all measured at position 2. Points × refer to Re = 390, ○ to Re = 600, □ to Re = 800, ● to Re = 1 000, and + Re = 1 300. The energy dissipating eddies are those for which $\kappa > 5 \times 10^3$.

(9)] was 0.48 × 10^{-3} m^2 s^{-3} at Re = 2 530, increasing to 0.2 m^2 s^{-3} at Re = 9 470.

The energy spectrum, as a function of wave number, is shown in Figure 6. Here, ψ^* is plotted as a function of the wave number κ on log-log scales. There is no extended linear region of the curve of slope −5/3 such as is found for flow over plates.

Eddies in Impinging Submerged Jet

For the submerged jet, impinging onto the gas-liquid surface, Figure 7 shows $\tilde{v}_x'x$ as a function of y. The multiplication of $\tilde{v}_x'$ by the radial distance x is merely to make it possible to represent the points on a simple graph. For this system, the Reynolds number is that of the water leaving the nozzle.

In this system, both $\tilde{v}_x'$ and $\bar{v}_x$ increase markedly as the interface is approached. Intensities of turbulence generally increased with depth y and with Re_n, for example, 33% at y = 1 mm and Re_n = 1 570 and 60% at Re_n = 3 370. The corresponding values were 54 and 100% at y = 4 mm.

The length scale l_L decreased markedly away from the surface, but it increased with Re_n, typical values (at y = 1 mm) being 3 to 15 mm over the range of Re_n. The corresponding length scale l_m was from 2 to 10 mm. P_M values close to the interface at x = 20 mm were in the range 0.002 to 3.8 m^{2}s^{-3}.

Spectra were similar to those for the stirred cell.

Eddies in Water Film Over Smooth Inclined Plate

The turbulence intensity was too low to measure below Re = 1 000. Here, Re is defined as the volumetric flow rate per unit breadth of the plate divided by ν.

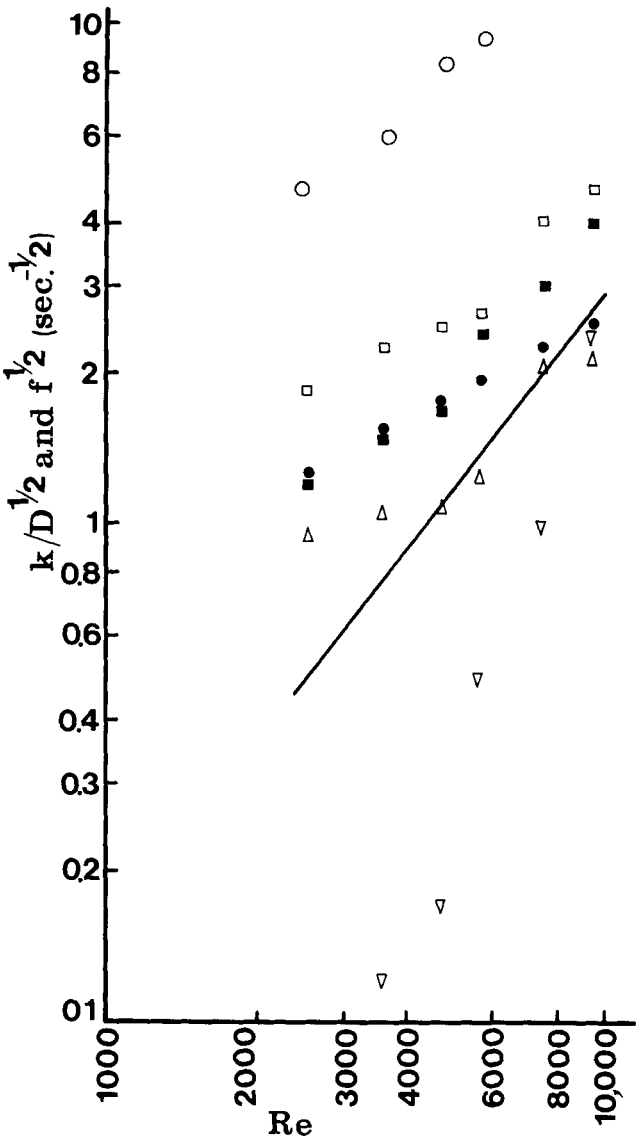

Fig. 10. Log-log plot of square root of eddy frequencies against Re for the stirred cell. Points are as follows: □ Equation (11), ● Prandtl frequencies Equation (12), ■ Prandtl frequencies based on mean experimental $\tilde{v}_x'$ near surface, △ Equation (15), ▽ Equation (16) using mean $\tilde{v}_x'$, ○ Kolmogoroff frequencies. The full line (of slope 1.3) represents the experimental $k/D^{1/2}$ results.

In this system, $\bar{v}_x$ was 0.83 m s^{-1} at Re = 1 000 and 0.98 m s^{-1} at Re = 1 300. Corresponding values of $\tilde{v}_x'$ were 0.076 and 0.162 m s^{-1}. The turbulence intensities were thus 9 and 17%.

The length scale l_L was 42 mm at Re = 1 000 and 23 mm at Re = 1 300. The scale l_M was 5 mm at both Re values. P_M was 0.010 and 0.18 m^2 s^{-3} at the two Reynolds numbers.

The energy spectrum (Figure 8) shows a range where the slope is close to −5/3.

Eddies in Water Film Over Rough Inclined Plate

In this system, turbulence was strong at Re values as low as 390. Re is defined as for the flow over the smooth plate, and values of 390, 600, 800, 1 000, and 1 300 were used.

The mean velocity $\bar{v}_x$ was much greater in position 2 than in the other positions. For example, at Re = 1 000, $\bar{v}_x$ in the four positions was 0.11, 0.74, 0.26, and 0.64 m

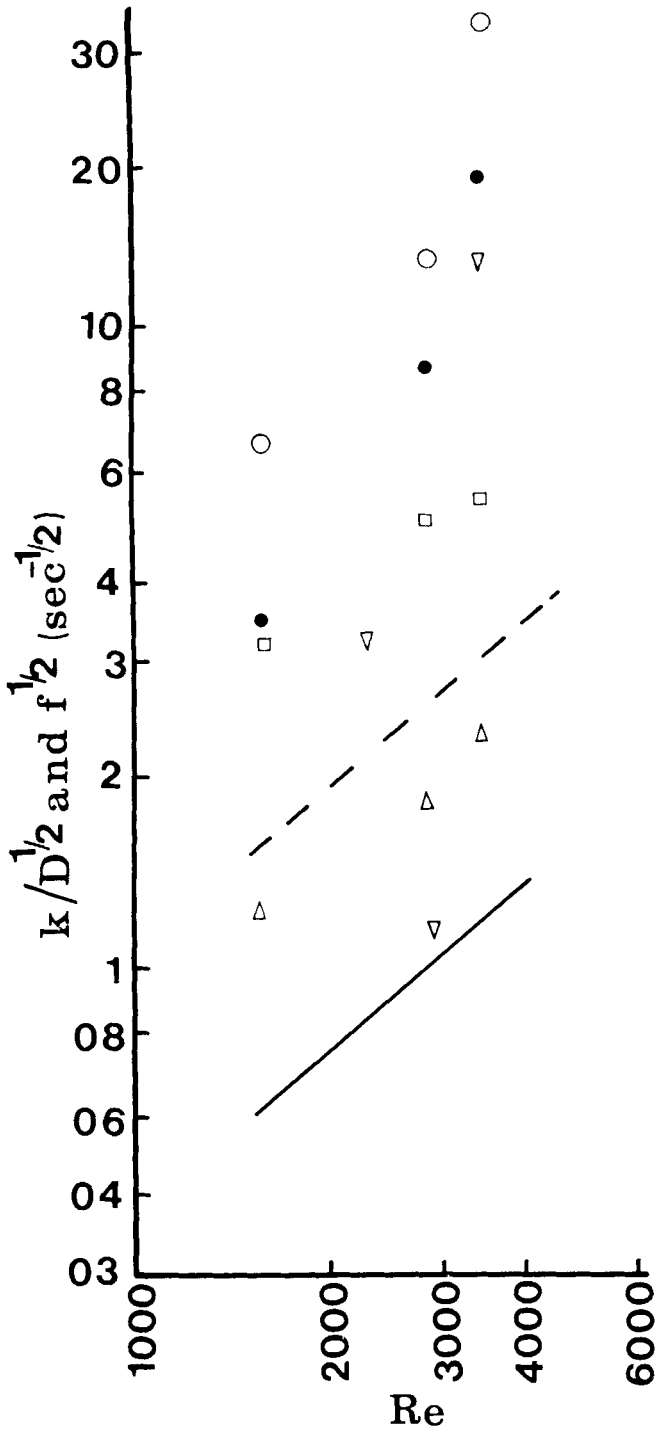

Fig. 11. Log-log plot of square root of eddy frequencies against Re for the impinging turbulent jets at x = 20 mm with the nozzle situated 60 mm vertically below the free surface. Points are as in Figure 10 except that ▽ now represents Equation (16) with $v' = \tilde{v}_x'$ as y tends to zero, and ● represents Prandtl frequencies calculated from Equation (13). The full line is the experimental overall $k/D^{½}$ data, and the broken line represents these data multiplied by 2.5.

s^{-1}. Corresponding values of $\tilde{v}_x'$ were 0.056, 0.29, 0.13, and 0.21. As with the mean velocities, v_x' is highest in position 2 and least in position 1. The corresponding turbulent intensities in positions 1 to 4 were, respectively, 50, 40, 50, and 30%.

The length scales l_L at the four positions (at Re = 1 000) were, respectively, 0.90, 4.1, 1.9, and 3.9 mm. The l_m values were, respectively, 0.6, 2.6, 1.4, and 2.3 mm.

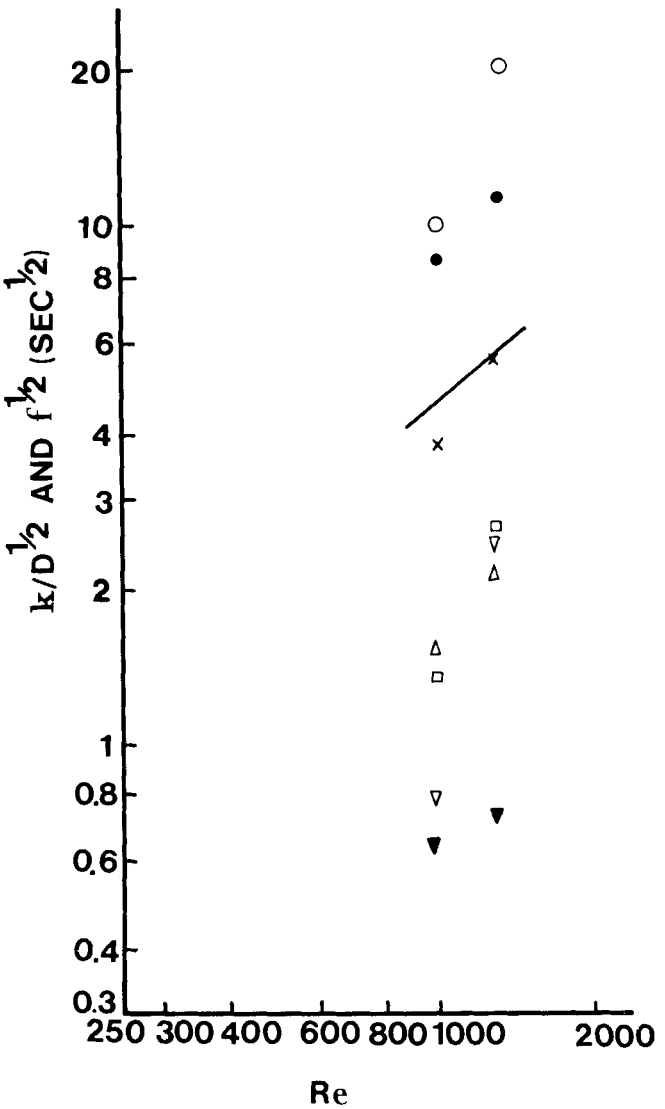

Fig. 12. Log-log plot of square root of frequency against Re for the smooth plate inclined at 24.3 deg to the horizontal. Line and points as in Figure 11, and also × represents Equation (11) using l_m, ▽ Equation (16) with $\tilde{v}_x'$ from experiment, ▼ Equation (16) with $v' = v_0$ from Equation (17), ● Prandtl frequencies with $l = B_f$.

P_M values were (at Re = 1 000) 0.1, 3.4, 0.5, and 1.5 ($m^2\ s^{-3}$) at the four positions.

The energy spectrum at position 2 is shown in Figure 9. There is clearly an appreciable range of slope −5/3.

Mass Transfer Rates

The overall mass transfer coefficient k for oxygen absorbing into the turbulent water at 25°C was divided by $D^{½}$ to obtain the full lines shown in Figures 10 to 13. The value of D used was $2.4 \times 10^{-9}\ m^2\ s^{-1}$.

The concentration fluctuation measurements in the stirred cell showed deviations from the hot wire results at eddy wave numbers greater than 400 m^{-1} (that is, frequencies greater than 10 Hz). Because of the poorer frequency response of the microelectrode, the values of l_L and l_m were somewhat greater (by a factor of about 1.3) than the values from the hot wire measurements. For water flowing over the smooth plate at Re = 1 000 and Re = 1 300, l_L appeared absurdly high, being 150 and 230 mm, respectively (compared with 42 and 23 mm from the hot wire measurements). The l_m values from concentration fluctuations were fourteen times too great.

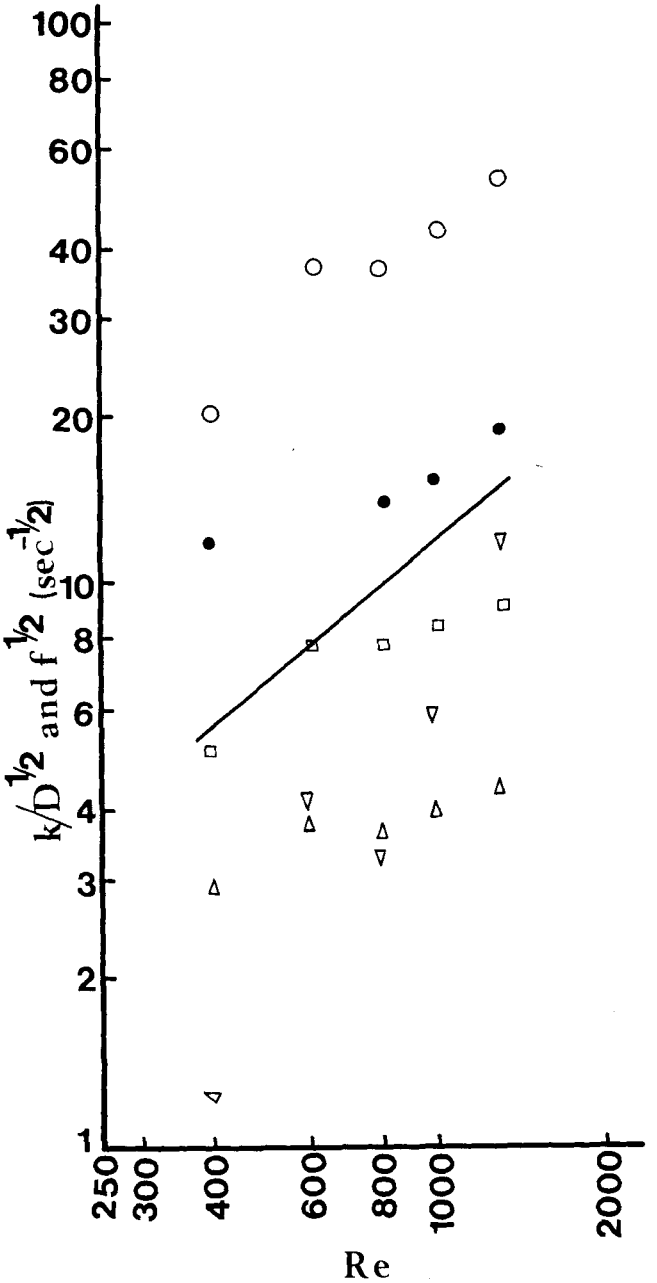

Fig. 13. Rough plate results, with points and line as in Fig. 12. All the eddy data refer to position 2.

We conclude that the eddy sizes and frequencies can be determined only by using hot wire probes, the microelectrodes are not sufficiently responsive to the high frequencies, and data from them are therefore not used in the present work.

DISCUSSION

Stirred Cell

That $\tilde{v}_x'$ shows no regular trend as y is varied (Figure 4) supports the use of Equations (1) and (2) for analyzing mass transfer rates at the free surface in a stirred cell. The observed ratio of $\tilde{v}_x'/NL$ of 0.20 can be compared with the ratio of 0.25 deduced by McManamey et al. (1975) from mass transfer rates when there were contrarotating stirrers in two liquid phases. The rotational flow in the present cell (and the different stirrer arrangement) is evidently responsible for the difference and also for our higher ratios at the fastest stirring speeds.

The extreme limits of the P_M values (at $y = 0.5$ mm) correspond to Kolmogoroff eddy sizes of 200 and 44 μm, that is, to wave numbers of 3×10^4 and 14×10^4 m^{-1}.

Figure 10 shows that Equation (11) gives frequencies that are much higher than $k/D^{1/2}$; that is, the eddies responsible for mass transfer are larger (of lower frequency) than the x directional macroscale.

The Prandtl frequencies [Equation (12) closed circles] are in closer accord with mass transfer rates, though $f_P^{1/2}$ is too great at the lower Reynolds numbers. Alternatively, f_P can be calculated from the mean $\tilde{v}_x'$ values (from Figure 4), taking the eddy length again as $0.3L$. These $f_P^{1/2}$ values are shown in Figure 10 by the full squares. Again, the eddy frequency is too high, but the slope is closer to that of the mass transfer data.

Equation (15), based on the Levich approach, gives the best agreement with mass transfer rates. In Figure 10, $f_y^{1/2}$ is shown by upright triangles. Thus, the y directional Prandtl eddies ($l = 0.4y$) gives the best agreement in magnitude and (except at the two lowest Reynolds numbers) good agreement with the slope against Re.

Equation (16), with v' substituted by the mean $\tilde{v}_x'$ (from Figure 4), gives results (inverted triangles) generally much too low and of too great a slope. By trial and error, however, one finds good agreement of Equation (16) with experiment if $v' = 0.7NL$ is substituted.

The Kolmogoroff eddies are clearly of very much higher frequency (that is, very much smaller) than corresponds to the mass transfer line.

We thus conclude from these comparisons that large eddies are responsible for most of the mass transfer. This conclusion is also consistent with the energy spectra. Figure 6 shows that much of the energy is in the largest eddies. The Prandtl eddies in the stirred cell are about 10 mm long, and if (in a slightly arbitrary way) band widths are assigned to the different classes of eddies, about 32% of the total eddy energy lies in the very large eddies, about 43% in the Prandtl range, about 21% in the macroscale range, about 3% in the dissipating range, and only about 1% in the Kolmogoroff range.

Impinging Submerged Jets

Here, $\tilde{v}_x'$ increases markedly as the interface is approached (Figure 7), as expected from the spreading of faster moving jet liquid over the bulk liquid. Thus, the assumption that $\tilde{v}_x'$ is independent of y is not justified in this particular system.

The measured k values are overall for the whole tank, but the frequencies we use for comparison are measured at $x = 20$ mm. From earlier work (Davies, 1966, 1972), it is known that the k values at $x = 20$ mm can be up to 2.5 times higher than the mean overall values, and in Figure 11 the experimental data for the mass transfer ratio $k/D^{1/2}$ (full line) has therefore been raised by 2.5 times to give the broken line, this latter corresponding to mass transfer in or near the impingement region.

Equation (11) gives results higher than this revised $k/D^{1/2}$ line, indicating that the eddies responsible for mass transfer are larger (that is, of lower frequency) than the x directional macroscale.

The mass transfer eddies also appear to be larger than the x directional Prandtl eddies [of length about 1.4 mm, as calculated from Equation (13)], using the experimental values of $\tilde{v}_x'$ extrapolated to zero y.

Equation (15) gives the triangles in Figure 11. They are in reasonable agreement with the experimental data (broken line).

Equation (16), with v' replaced by $\tilde{v_x}'$ extrapolated to zero y, is unsatisfactory (inverted triangles) because the calculated $k/D^{1/2}$ increases so steeply with Re.

The Kolmogoroff eddies are clearly of much higher frequency than those responsible for mass transfer (and the slope is too great).

Water Film Over Smooth Inclined Plate

The large integral length scales (up to 42 mm) suggest that waves are responsible for much of the turbulence at the Reynolds numbers concerned.

The large range of eddy sizes leads, however, to a considerable region of the spectrum (Figure 8) in which the slope is $-5/3$, suggesting a large inertial subrange. To check this, Equation (7) may be used. With P_M obtained from Equation (9) as 0.010 $m^2\ s^{-3}$ at $Re = 1\,000$ and with κ taken as 400 m^{-1}, Equation (7) gives $\psi = 3.1 \times 10^{-6}\ m^3\ s^{-2}$. This is then equated to $(\tilde{v_x}')^2\psi^*$, whence ψ^* is calculated to be 5.4×10^{-4} m, corresponding satisfactorily with the experimental value (Figure 8) of 4×10^{-4} m.

The Kolmogoroff eddy lengths are 92 and 45 μm at the two Reynolds numbers.

The ratio $\tilde{v_x}'/v_o$ can now be checked, v_o being the shear stress velocity, which at $Re = 1\,000$ is 0.065 m s^{-1} (Davies, 1972). The ratio $\tilde{v_x}'/v_o$ is then 1.17, and since the mass transfer coefficient varies as $(v')^{3/2}$, the previously calculated $k/D^{1/2}$ (Davies, 1972) should be increased by a factor of 1.26. The calculated figure (based on the x directional fluctuation) is now 0.81 $s^{-1/2}$, still lower than experimental result of 3.1 s^{-1}.

In Figure 12, the experimental results of $k/D^{1/2}$ are compared with the various eddy frequencies. Equation (11) gives frequencies which are too low, the reason being that the x directional eddies are very large in this system (l_L is 42 and 23 mm, respectively, at $Re = 1\,000$ and $Re = 1\,300$). These large eddy lengths are evidently related to the gravity waves on the surface of the liquid, which is in the transitional regime at these Reynolds numbers. Better agreement is obtained by replacing l_L in Equation (11) by the microscale eddy length l_m (5.3 and 5.1 mm at the two Reynolds numbers), though this agreement may be coincidental.

The Prandtl frequencies calculated for the y direction from $l = 0.1\ B_f$ are high (order of 1 000 s^{-1}, that is, $f_P^{1/2} \sim 32\ s^{-1/2}$). Even if we put $l = B_f$, $f_P^{1/2}$ is 10 $s^{-1/2}$, still higher than the experimental $k/D^{1/2}$. It thus appears that surface renewal involves eddies intermediate in size between the x and the y directional large eddies.

Equation (15) gives results similar to Equation (11) and for the same reasons as listed above. Since we have not extrapolated to zero y in this system, Equation (15) is of limited validity here.

Equation (16) gives results rather too low if the experimental $\tilde{v_x}'$ is substituted (inverted open triangles in Figure 12) and still lower (inverted full triangles) if v_o is substituted into Equation (16) from Equation (17). Evidently the specialized form of turbulence associated with the surface waves is particularly effective for mass transfer.

The Kolmogoroff eddies are clearly of a much higher frequency than is consistent with the mass transfer results.

From the spectrum of eddy energies (Figure 8), it can be calculated that the largest x directional eddies contain about 57% of the turbulent energy. That they do not apparently control mass transfer rates may be due to their moving the surface bodily without causing surface renewal. The macroscale x directional eddies contain about 37% of the turbulence energy and the dissipating (microscale) eddies about 6%. The Kolmogoroff eddies have negligible energy by comparison.

The conclusion from Figure 12 is that mass transfer depends principally on large eddies, intermediate in size between the x directional and the y directional Prandtl eddies.

Water Film Over Rough Inclined Plate

Here there is a pronounced inertial subrange of eddies, as seen from the region of slope $-5/3$ in Figure 9. The turbulence energy is clearly being cascaded through this equilibrium range before being dissipated by viscosity.

The flow pattern here is of the wake interference type, and an intensely fluctuating appearance is visible on the surface of the liquid film under these conditions. The value of P_M at position 2 varied from 0.2 m^2 s to 7.8 $m^2\ s^{-3}$ over the range of Reynolds numbers corresponding to l_K values of 44 and 18 μm.

One can again use Equation (7) to check that the slope of $-5/3$ in Figure 9 is significant and that Equation (9) is, for our systems, a reasonable method to deduce P_M. Thus, for position 2 at $Re = 1\,000$, $P_M = 3.4\ m^2\ s^{-3}$. Hence, for $\kappa = 2 \times 10^3\ m^{-1}$, Equation (7) gives $\psi = 10.4 \times 10^{-6}\ m^3\ s^{-2}$; that is, ψ^* is 1.3×10^{-4} m. The experimental value (Figure 9) is 1.6×10^{-4} m.

The eddy pattern over the roughness elements is clear from the velocity fluctuations in the different positions. For this particular height to spacing ratio, the velocity fluctuations (that is, the eddy movements) are much faster in position 2 and much slower in position 1. Incidentally, the smaller slower eddies in position 1 (in the so-called separation vortex) will therefore be favorable for any solid suspended particles to be deposited. On an initially smooth surface on which deposition is occurring, a band or ripple deposition will thus be stable, since some slight chance initial deposition in a band will favor further deposition in the region of that band.

To obtain $\tilde{v_x}'/v_o$, we use the value of $v_o = 0.071$ m s^{-1} (from Davies, 1972, pp. 199, 203). This gives velocity ratios of 0.8, 4.1, 1.8, and 3.0 in positions 1, 2, 3, and 4 at $Re = 1\,000$, confirming (at least for the x directional fluctuations) that in wake interference turbulence this velocity ratio may be as high as 4, as surmized previously (Davies, 1972) from mass transfer results.

As Figure 13 shows, the x directional macroscale frequencies at position 2 give [by Equation (11)] good agreement with the experimental mass transfer data, though these eddies appear to be rather too large at high Re values. The l_L values are practically independent of Re at positions 1, 2, and 3, though at position 4 they increase slightly with Re. These findings are in contradiction to the assumption of Brumfield et al. (1975) whose assumptions led to a postulated decrease of l_L as Re is increased.

Prandtl frequencies in the y direction, calculated from $l_P = 0.1e$, are much too high. With $l_P = B_f$, the $f_P^{1/2}$ values (again for position 2) are still somewhat higher than the mass transfer figures.

Equation (15) gives results too low, again possibly because of the x directional fluctuations being greater than those in the y direction, and also because we were not able to extrapolate to zero y.

Equation (16) gives low results (again for $\tilde{v_x}'$ in position 2, inverted open triangles on Figure 13) at the lower Re values. With v_o (from Davies, 1972) substituted into

Equation (16), the result (not shown here) is still lower.

The Kolmogoroff frequencies are clearly much too high to relate to mass transfer.

The eddy spectrum (Figure 9) indicates that about 47% of the eddy energy is in the largest eddies, about 45% in the macroscale range, with only about 8% in the microscale (dissipating) range, and a negligible contribution from the Kolmogoroff eddies.

Thus, in this system, most of the mass transfer is apparently controlled by the macroscale eddies, these being larger than the y directional Prandtl eddies but smaller than the measured x directional eddies.

NOTATION

B_f = thickness of liquid film, m or mm
D = molecular diffusivity, $m^2\ s^{-1}$
D_E = eddy diffusivity, $m^2\ s^{-1}$
e = height of roughness elements, m or mm
f = frequency, s^{-1}
g = gravitational acceleration, $m\ s^{-2}$
k = mass transfer coefficient, $m\ s^{-1}$
l_K = Kolmogoroff eddy length, m or mm
l_L = macroscale of eddies, m or mm
l_m = microscale of eddies, m or mm
l_P = Prandtl eddy length, m or mm
L = tip-to-tip length of stirrer blade, m or mm
N = number of revolutions per second of stirrer, s^{-1}
P_M = power per unit mass of liquid, $m^2\ s^{-3}$
$Q(t)$ = velocity autocorrelation coefficient with respect to time, $m^2\ s^{-2}$
$Q^*(t) = Q(t)/(\tilde{v_x}')^2$, dimensionless
Re = Reynolds number
s = frequency of surface renewal, s^{-1}
s_1, s_2 = distances as in Figure 3
t = time, s
t_L = eddy macrotime scale, s
$\bar{v}_x$ = mean local velocity in x direction, $m\ s^{-1}$
v_x' = fluctuation velocity in x direction, $m\ s^{-1}$
$\tilde{v}_x'$ = root mean square fluctuation velocity in x direction, $m\ s^{-1}$
v_y' = fluctuation velocity in y direction, $m\ s^{-1}$
$\tilde{v}_y'$ = root mean square velocity fluctuation in y direction, $m\ s^{-1}$
v_o = shear stress velocity, $m\ s^{-1}$
x = distance in direction of flow, m or mm
y = distance normal to surface measured into the water, m or mm

Greek Letters

θ = angle of inclination of plate to horizontal
κ = eddy wave number [$= 2\pi/$(eddy length)], m^{-1}
ν = kinematic viscosity of water, $m^2\ s^{-1}$
$\phi^*(f)$ = normalized one-dimensional energy function (of frequency), s
ψ = energy function (of wave number), $m^3\ s^{-2}$
ψ^* = normalized energy function (of wave number), m

Overbars

— = time averaged value
~ = root mean square
' = fluctuations

Subscripts

K = Kolmogoroff eddies
L = macroscale
M = per unit mass
m = microscale
P = Prandtl eddies
x = x directional
y = y directional
0 = in shear stress region close to surface

LITERATURE CITED

Banerjee, S., D. S. Scott, and E. Rhodes, "Mass Transfer to Falling Wavy Liquid Films in Turbulent Flow," *Ind. Eng. Chem. Fundamentals*, **7**, 22 (1968).

Brumfield, L. K., R. M. Houze, and T. G. Theofanous, "Turbulent Mass Transfer at Free, Gas-Liquid Interfaces with Application to Film Flows," *Intern. J. Heat Mass Transfer*, **18**, 1077 (1975).

Bungay, H. R., M. Y. Huang, and W. M. Sanders, "Quantitation of Eddy Diffusion using an Oxygen Microelectrode," *AIChE J.*, **19**, 373 (1973).

Danckwerts, P. V., "Significance of Liquid-Film Coefficients in Gas Absorption," *Ind. Eng. Chem. Process Design Develop.*, **43**, 1460 (1951).

Davies, J. T., "Interfacial Renewal," *Chem. Eng. Progr.*, **62**, No. 9, 89 (1966).

———, *Turbulence Phenomena*, Academic Press, New York (1972).

Fortescue, G. E., and J. R. A. Pearson, "On Gas Absorption into a Turbulent Liquid," *Chem. Eng. Sci.*, **22**, 1163 (1967).

Hinze, J. O., *Turbulence*, 2 ed., pp. 106-111, McGraw-Hill, New York (1975).

Jeffries, R. B., D. S. Scott, and E. Rhodes, "Structure of Turbulence Close to the Interface in the Liquid Phase of a Co-Current Stratified Two-Phase Flow," *Proc. Inst. Mech. Engrs.*, **184**, No. 3C, 204 (1969).

Kataoka, H., and T. Miyauchi, "Effects of Physical Properties and of Turbulence on the Rate Coefficient of Mass Transfer at the Free Surface of Agitated Vessels in Turbulent Region," *Kagaku Kogaku*, **36**, 888 (1972).

Lamont, J. C., and D. S. Scott, "An Eddy Cell Model of Mass Transfer into the Surface of a Turbulent Liquid," *AIChE J.*, **16**, 513 (1970).

Levich, V. G., *Physicochemical Hydrodynamics*, Prentice Hall, Englewood Cliffs, N.J. (1962).

Lozano, F. J., "Turbulence and Mass Transfer," Ph.D. thesis, Univ. Birmingham, England (1976).

Lumley, J. L., "Interpretation of Time Spectra Measured in High-Intensity Shear Flows," *Phys. Fluids*, **8**, 1056 (1965).

McManamey, W. J., J. T. Davies, J. M. Woollen, and J. R. Coe, "The Influence of Molecular Diffusion on Mass Transfer between Turbulent-Liquids," *Chem. Eng. Sci.*, **28**, 1061 (1973).

McManamey, W. J., S. K. S. Multani, and J. T. Davies, "Molecular Diffusion and Liquid-Liquid Mass Transfer in Stirred Transfer Cells," *Chem. Eng. Sci.*, **30**, 1536 (1975).

Miyauchi, T., and H. Kataoka, "Liquid Film Coefficient of Mass Transfer on Free Liquid Surface," *J. Chem. Eng. Japan*, **3**, 257 (1970).

Prasher, B. D., "Gas Absorption into a Turbulent Liquid," *Chem. Eng. Sci.*, **28**, 1230 (1973).

———, and G. B. Wills, "Mass Transfer in an Agitated Vessel," *Ind. Eng. Chem. Process Design Develop.*, **12**, 351 (1973).

Ruckenstein, E., "Physical Models for Mass or Heat Transfer Processes," *Intern. Chem. Eng.*, **7**, 490 (1967).

Taylor, G. I., "The Spectrum of Turbulence," *Proc. Royal Soc.*, **A164**, 476 (1938).

Tennekes, H., and J. L. Lumley, *A First Course in Turbulence*, pp. 20, 66-69, 265, M.I.T. Press, Cambridge, Mass. (1972).

Tsao, G. T., and D. D. Lee, "Oxygen Transfer in Fermentation," *AIChE J.*, **21**, 979 (1975).

Manuscript received August 8, 1977; revision received March 13, and accepted November 6, 1978.